Metallurgical and Materials Engineering *Review paper*
Association of Metallurgical Engineers of Serbia AMES *https://doi.org/10.30544/400*

HARD TEMPLATE SYNTHESIS OF NANOMATERIALS BASED ON MESOPOROUS SILICA

Slavica M. Savić[1], Katarina Vojisavljević[2], Milica Počuča-Nešić[2], Kristina Živojević,[1] Minja Mladenović,[1] Nikola Ž. Knežević[1]*

[1]Biosense Institute, University of Novi Sad, Zorana Đinđića 1, 21000 Novi Sad, Serbia
[2]Institute for Multidisciplinary Research, University of Belgrade, Kneza Višeslava 1a, 11030 Belgrade, Serbia

Received 23.11.2018
Accepted 11.12.2018

Abstract

Diverse hard template synthetic methodologies are being employed for the synthesis of mesostructured metal oxide and carbon nanomaterials, with the application of mesoporous silica as the hard template. We describe the main differences and advantages/disadvantages between the soft and hard templated synthetic routes, provide an overview of the synthesis and characteristics of different templating mesoporous silica nanomaterials and discuss on practical aspects of the hard template synthetic methodology for obtaining various metal-oxide and carbon-based mesostructured nanomaterials. Also, we cover various recent applications of thus constructed mesostructured metal oxide and carbon nanomaterials, such as sensing, energy storage, fuel cells, and catalysis, which demonstrate the highly promising character of the hard template methodology for the synthesis of a new generation of nanomaterials with broad application potential.

Keywords: Mesoporous silica; mesostructured iron oxide; mesostructured carbon; nanomaterials synthesis.

Introduction

A plethora of synthetic methodologies are being employed for the construction of mesoporous materials. Two of the most common strategies are “soft”-templating and “hard”-templating (“nanocasting”) methods [1, 2]. The templated syntheses of nanostructured materials typically entail the following three consecutive steps: template preparation, template-directed synthesis of the target materials (via sol-gel, precipitation, hydrothermal synthesis, and so forth) and finally the template removal.

* Corresponding author: Nikola Knežević, *nknezevic@biosense.rs*

The "soft" templating methodology refers to a direct synthesis of the porous materials, with block copolymers or surfactants being employed as structure directing agents (SDAs) and addition of precursors (e.g., metal salts for metal oxide (MOX) nanomaterials or triethoxysilane and organosilanes for SiO_2-based nanomaterials) leading to the construction of the desired mesostructured nanomaterial. Nanoparticles are formed through inter- and intramolecular interactions between SDAs and molecular precursors (chemical, hydrogen bonding, electrostatic interactions). Morphology of the mesoporous materials greatly depends on the character of interactions at the organic-inorganic interface. In case of application of a cationic surfactant, e.g., cetyltrimethylammonium bromide, in a strongly alkaline environment, an electrostatic attraction exists between the positively charged surfactant headgroup and negatively charged molecular precursor, while in a strongly acidic environment, the interaction between the organic and inorganic interface is established by weak hydrogen bonding. Thus, inorganic species at the interface polymerize, cross-link and assemble with the help of surfactants [1].

The soft templating method relies on cooperative self-assembly of the surfactant and the precursor to form a mesoporous structure. The process is based on the interactions between inorganics and surfactants which assemble into inorganic-organic mesostructured composites *in situ*, which is well discussed in the literature [3-8]. The mesoporous structure of the final material is obtained after removal of the pore-templating surfactant by low-temperature calcination (up to 600 °C) or by different washing techniques.

The "nanocasting" process is analogous to the macroscopic procedure used in metallurgy (called "casting") where the matrix (template) acts as the "casting mold" and the product (replica) being the "cast". When the scale in the process is minimized to nanometric size, it can be termed as "nanocasting". This way it can be used as a promising strategy for the syntheses of nanoporous carbons, metals, and MOXs. Hard-templating is a facile synthetic method for fabrication of porous materials with a stable porous structure by depositing the targeted materials into the confined spaces of the template, resulting in a reverse replica of the mold. The structure replication is very straightforward and this approach utilizes porous ''hard templates'' (usually mesoporous silica or carbon). The pores of these templates are impregnated with a precursor compound for the desired product (e.g., a metal salt for MOX) which is then thermally converted to the product *in situ*. The template is finally removed to yield the desired mesoporous material as a negative structural replica of the hard template.

Soft vs. hard templated synthesis

One of the significant disadvantages of the soft templating process is poor control over the condensation reaction, as it relies on sol-gel chemistry where the final product is quite dependent on the laboratory conditions (temperature, pH, humidity) [9, 10]. Narrow temperature range during synthesis favors low crystallinity and therefore, the material obtained by soft templating method yields in amorphous or semicrystalline phase. Depending on the desired application of the mesostructured product, the presence of amorphous phases can have negative effects, such as facilitating the recombination of electrons and holes, decreasing the catalytic efficiency and/or reducing the conductivity of the material, which limits the electronic applications of the material. Even though the

amorphous phase can be eliminated during the calcination process, the mesoporous structure cannot be well-preserved after the high-temperature thermal treatment.

Significant advantage of the soft templating method, in general, is the simplicity of the one-step synthetic procedure for obtaining mesostructured materials and simple removal of the templating surfactant, in comparison to the more complex hard templating method with the requirement for removal of silica mold [11-13, 1]. Over the past two decades, various researchers embarked on the templated synthesis approach to obtain mesoporous MOXs with highly ordered structures, high surface area, and different porosity. A number of mesoporous MOX materials are produced through the so-called "soft templates", i.e. by self-assembled supramolecular aggregates of amphiphiles, which serve as structure directing agents [7, 8] For example, *Hoa et al.* successfully used soft templating for the fabrication of mesoporous nanoplate-like monoliths of tungsten oxide with large specific surface area and high crystallinity for NO_2 sensing [14].

One of the main advantages of the process in the case of the synthesis of mesoporous MOXs is that many ordered metal oxides cannot be prepared by single "soft" templating using amphiphilic SDAs because of their tendency to phase separate from SDA species to form pure crystalline, nonporous phase.

Contrary to the soft templating method which involves complicated sol−gel chemistry, where the mesostructure of the final product can be quite sensitive to the experimental conditions (temperature, pH, humidity) and the condensation process of the metal precursors has to be well controlled to avoid amorphous or semicrystalline phase, the hard template method has many advantages such as controllability, pore regularity, and crystallinity [15-17]. Various types of mesoporous MOXs have been successfully prepared using the nanocasting method [15, 16, 18] and many of them have been developed using mesoporous silica templates [19-25].

Mesoporous silica as hard template has attracted considerable attention of the scientific community owing to its well-ordered structure, high surface area, uniform pore distribution, high thermal stability, low toxicity, permeability and excellent compatibility with other materials [25]. All of these silica's unique properties can be easily tuned by varying the experimental conditions (changing SDAs, hydrothermal conditions, and so forth). What gives silica a plain advantage as a hard template over other possible hard templates for MOX synthesis, such as carbon, is strengthening the interaction between metal precursors and silica over surface silanol groups (Si-OH). Ordered mesoporous carbon has poor surface wetting and solution infiltration which can limit the uniform dispersion of metal precursors and the quality of the replica itself [23]. The other advantages of silica are its thermal stability, chemical inertness and good crystallinity of obtained replicas at high temperatures. Bearing in mind that material obtained by the soft templating, using heavily controlled sol-gel chemistry, consists mainly of the amorphous phase, the replicated MOXs obtained by hard templating are characterized with good crystallinity thanks to the thermal stability of the silica template. However, the template removal (leaching) is one of the main downsides of the hard templating process, since it has to be removed with either HF or NaOH. This significantly limits the applicability of this methodology as some of the MOXs such as ZnO, MgO, Al_2O_3 can react with leaching agents [25]. Besides, comparing to the soft templating, the hard template method is time-consuming since even the preparation of the template itself can be up to a few days long.

Synthesis of mesoporous silica templates

The synthesis of mesoporous silica particles dates back to 1990s, when the Mobil Oil Company primarily developed MCM-41 silica with a 2D hexagonal pore arrangement (space group: *p6mm*), and later on, a series of well-ordered mesoporous silica known as M41S, including MCM-48 with a 3D cubic pore arrangement (space group: $Ia\bar{3}d$). The synthesis of these materials relies on modified Stöber process [26], i.e. soft-templating strategy where inorganic-organic mesostructured composites are formed from a silica precursor (usually tetraethyl-orthosilicate, TEOS) and supramolecular aggregates of ionic surfactants (long-chain of alkyltrimethylammonium halides) as SDAs under necessary conditions [27-29]. Depending on the surfactant quantity, two mechanisms can occur in M41S formation:

- *a true liquid-crystal templating* (TLCT) in a sufficiently high concentration of surfactant, where a lyotropic liquid-crystalline phase forms under prevailing conditions (strictly defined temperature and pH) independently from the presence of the silica precursor, and
- *a cooperative mechanism* at a low concentration of surfactant, where a liquid crystalline phase forms through cooperative self-assembly between micelles and already added silica precursor.

Once the hydrolysis-condensation reactions are completed and an inorganic-organic composite is formed, the removal of surfactant by the acidic extraction or calcination results in mesoporous silica template. Both mechanisms involved in the formation of MCM-41 are schematically presented in Figure 1.

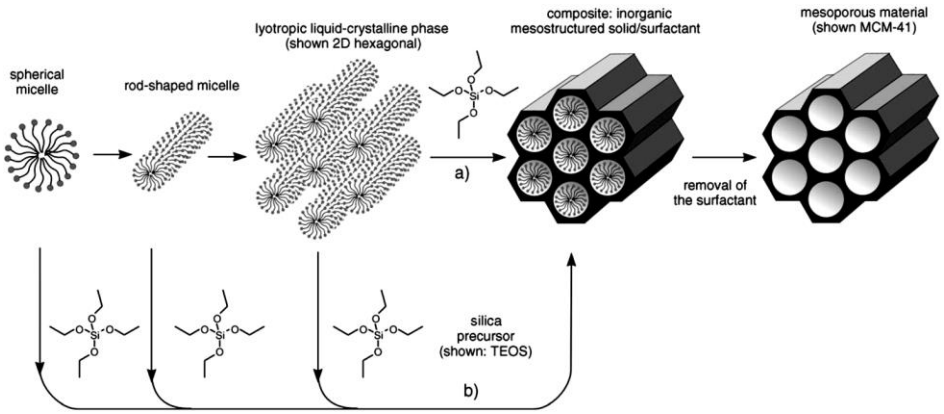

Fig. 1. Formation of mesoporous silica template through a true liquid-crystal templating a) and a cooperative self-assembling mechanism b). Reprinted with permission from (Hoffmann et al. 2006, [27]). Copyright 2006 Wiley-VCH Verlag GmbH & Co. KGaA, Weinheim.

The M41S class of silica has good thermal stability, high surface area and volume, well-defined pore topology with narrow pore size distribution and relatively small diameter of pore openings in the range 2 nm < D < 5 nm. Further investigation performed by other research groups [30-32], showed that variations induced in original synthesis approach could have a tremendous impact on the processing of the high-quality mesoporous materials with desired structure, controllable pore width (5 nm < D

<30 nm) and wall thickness (3 - 6 nm). For instance, an introduction of non-ionic SDAs, such as triblock copolymers (Pluronic 123, Pluronic 127,etc.) instead of ionic ones, switching from basic to acidic synthesis conditions, adding swelling agents (1,3,5-trimethylbenzene (TMB), polypropylene glycol (PPG), etc.) or using different maturation temperatures during formation of the mesophase leads to the formation of a several well-known families of mesoporous silica: SBA-n (SBA-15 - hexagonal structure, space group: *p6mm*; SBA-16 -body-centered cubic structure, space group: $Im\bar{3}m$), KIT-n (KIT-5: cage-like face-centered cubic structure, space group: $Fm\bar{3}m$; KIT-6: body-centered cubic structure, space group: $Ia\bar{3}d$) and FDU-n (FDU-1: body-centered cubic structure, space group: $Im\bar{3}m$; FDU-12: face-centered cubic structure, space group: $Fm\bar{3}m$). Some of them are illustrated in Figure 2.

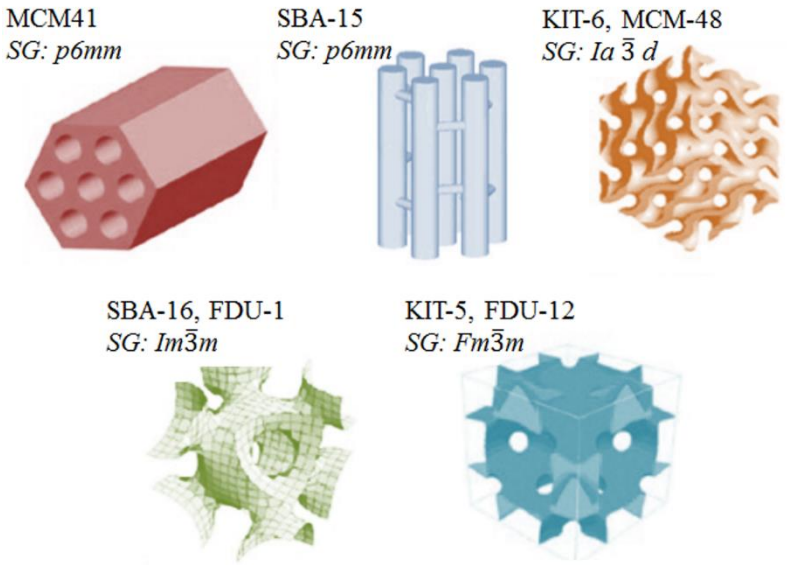

Fig. 2. Different types of mesoporous silica particles.

Hard template synthesis of mesostructured nanomaterials

Practical aspects of the hard template synthetic methodology

Endotemplating ("soft" templating) and exotemplating ("hard" templating or nanocasting) present two categories of templating approaches for the synthesis of ordered mesoporous materials including various transition and complex metal oxides.

Having in mind that the "soft" templating in not very applicable for the synthesis of the most of MOXs, the nanocasting was proposed as an ideal solution for the fabrication of ordered mesoporous materials. In general, an ordered mesoporous solid, usually silica prepared by the "soft" templating method, provides the porous matrix which is filled up with the precursor for MOX formation [25, 33]. Besides being a template for the processing of mesoporous MOXs, the mesoporous silica can additionally serve for the fabrication of mesostructured carbon material, which can be

used for various practical applications or further applied in metal oxide processing. Thermal treatment of the template-casted metal salts leads to conversion of the precursors to metal oxide, which forms MOX structure as a negative replica of the morphology of templating porous silica, after removal of silica mold by leaching with NaOH or HF solution. The entire process is named as a repeated templating mechanism [34], and it is schematically presented in Figure 3.

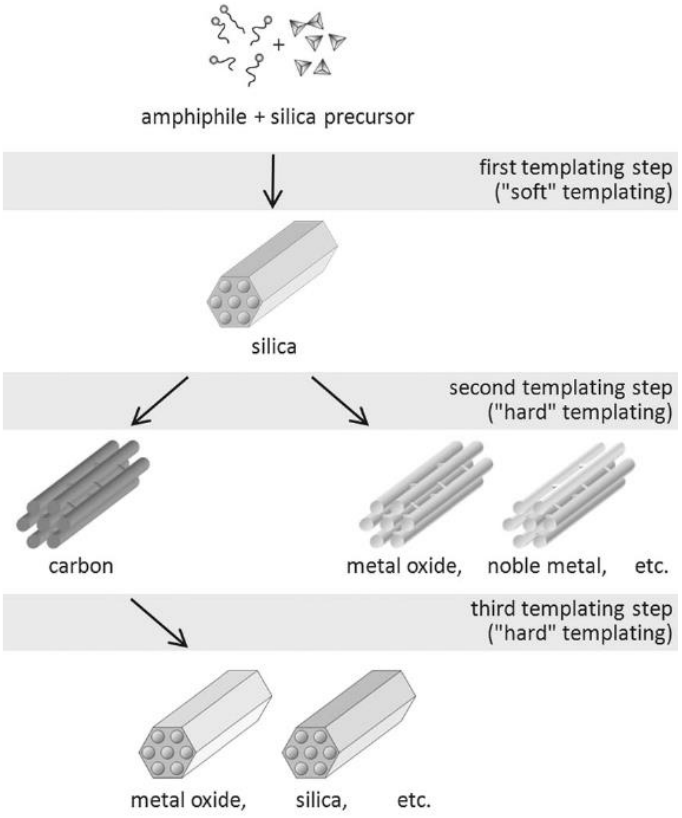

Fig. 3. A repeated templating mechanism involved in the processing of ordered mesoporous materials. Reprinted with permission from (Tiemann et al. 2008, [34]). Copyright 2008 American Chemical Society.

For the successful processing of the replica with an ordered mesoporous structure by the nanocasting, several points must be taken into consideration:

- as a precursor has to be selected a material which does not chemically react with the template (usually n-hydrates of metal salts, such as nitrates and chlorides);
- strong interactions between the precursor and the template should be avoided since they can result in accumulation of the precursor near the pore entrance leading to the pore blocking;

- the correct choice of the solvent can help in pore filling; for example, ethanol as a polar solvent possesses the amphiphilic property compatible to the silica pore wall surface, which enhances the capillary force and makes diffusion of precursor through the pores easier;
- for complete cross-linking of the material inside the pore system of the template, a sufficient amount of the precursor is needed (pore filling percentage: 5-15 %). Extremely high or too low percentage of pore filling can lead to the structure collapse of MOX after removal of the template.

Obviously, the most important step of the nanocasting is an infiltration of the precursor into the porous template matrix. For that purpose, wet impregnation, incipient wetness, dual-solvent or solid-liquid methods are usually used. In wet impregnation [35], a precursor previously dissolved in a solvent is added to the dilute suspension of the template. With continuous stirring, the precursor diffuses into the pores of the template and adsorbs on the pore walls. In order to fill the pores up to the desired value, several impregnation cycles must be performed.

In contrast to the wet impregnation, an incipient wetness method [36] utilizes a saturated precursor solution of the same volume as the pore volume of the template during impregnation. Therefore, this procedure minimizes the amount of the precursor material on the external surface of the template. Dual-solvent [20] method is a variant of the wet impregnation method. The difference is that in the dual-solvent method the template is dispersed in a non-polar solvent and mixed with a saturated aqueous solution of the precursor. As a result, the filling efficiency of the porous channels and homogeneity of the products is typically improved. If the melting point of the precursor is lower than its decomposition temperature, the solid-liquid method [37] can be used for its infiltration into the matrix, without the use of any solvent. Upon heating the mixture of the template and the precursor, once when the system reaches the melting point, the precursor converts to the liquid phase and enters the pores through the capillary forces.

Removal of the template is also an essential and delicate step in the processing of the mesoporous materials by nanocasting. To prevent the collapse of the mesoporous structure of MOX, the harsh conditions of the template removal by the chemical treatment with HF and extremely concentrated NaOH solutions ($c_{solution}$ > 2 M) must be avoided.

Complex metal oxides by nanocasting approach

Mesoporous silica templates have been demonstrated for the synthesis of materials with high specific surface area, narrow pore size distribution and large pore volume. *Wang et al.* [38] used KIT-6 template for the preparation of a series of mesoporous $LaFe_xCo_{1-x}O_3$ ($0 < x < 1$) perovskite-based materials with ordered mesoporous structure. Their pore structure parameters, in dependence of *x*, are: a specific surface area in the range of 270 – 119 m^2g^{-1} (BET), the pore size in the range of 7.0 – 10.1 nm (BJH) and pore volume in the range of 0.60 – 0.34 cm^3g^{-1}. All of these parameters are much higher in comparison with powders of the same composition prepared by conventional citrate route and are crucial for their applicability. Especially, $LaFe_{0.4}Co_{0.6}O_3$ showed higher electrochemical catalytic activity in Oxygen Reduction Reaction (ORR) owing to the electrical conductivity and existence of Fe^{2+}/Fe^{3+} redox couple.

Because of its semiconducting properties, undoped lanthanum ferrite ($LaFeO_3$) could not be used as the catalyst in ORR, but it was applicable in catalytic removal of Volatile Organic Compounds (VOCs) [39]. One step nanocasting process with the same preparation method as for the aforementioned $LaFe_xCo_{1-x}O_3$ was used for the preparation of $LaFeO_3$, with SBA-15 as the template. The procedure involved mixing precursors, crystal hydrates of lanthanum(III) nitrate, iron(III) nitrate and citric acid, with SBA-15 in *n*-hexane. After completing the reaction process and removing the silica template with 2 M NaOH (three times for 4 hours), the final mesostructured $LaFeO_3$ was obtained. The TEM analysis of the obtained material showed parallel nanowired structure inherited from SBA-15 template (Figure 4). In comparison to the sol-gel synthesized analogs, hard template-synthesized $LaFeO_3$ proved to have superior characteristics, having a specific surface area of 158 m^2g^{-1} (8 times higher than sol-gel prepared), with relatively narrow pore size distribution at ca. 5.5 nm. Also, the hard template-synthesized mesostructured $LaFeO_3$ showed improved catalytic properties for the process of methyl chloride oxidation, in comparison to classically synthesized one.

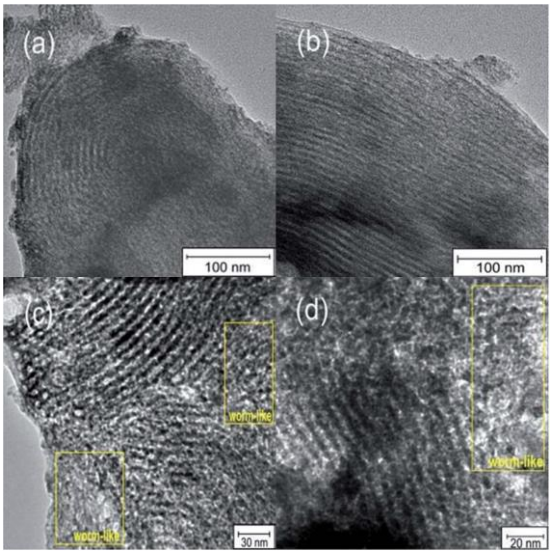

Fig. 4. TEM images of Meso-La-Fe-perovskite ((a): x97 000; (b): x97 000; (c): x145 000; and (d): x150 000). Reprinted with permission from (Zhang et al. 2014, [39]). Copyright 2014 The Royal society of Chemistry.

An additional proof that materials synthesized by hard template methods have better catalytic properties can be found in the case of Ni/La_2O_3 catalyst for dry reforming of methane [40]. In the first step of the synthesis, SBA-15 was used as the template for the synthesis of perovskite $LaNiO_3$ (LNO). After the calcination of the LNO/silica composite at 700 °C for 6 h and removal of the template, the as-prepared LNO mesoporous material was reduced at 700 °C for 2 h, to prepare the final product, Ni/La_2O_3. Both products, mesoporous LNO and reduced one, had a larger specific surface area compared to their classically synthesized counterparts and narrow pore size distribution. It is worth mentioning that after the second thermal treatment during the reduction process, the specific surface area was reduced from 150 m^2g^{-1} (mesostructured

LNO) to 50 m^2g^{-1}(Ni/La_2O_3), while the porosity retained its narrow distribution with a slight increase of the pore size after the reduction process. As expected by analyzing the catalytic performances of all prepared materials, it was concluded that catalysts obtained from the nano casted $LaNiO_3$ are highly useful for applications in the dry reforming process.

Materials with spinel structure can be also synthesized using hard template synthesis method. Synthesis of $NiFe_2O_4$ and $CuFe_2O_4$ was conducted by dispersing hydrated metal nitrates in stoichiometric proportion with silica templates (SBA-15, KIT-6, and MCM-48) in *n*-hexane [41]. After filtration, the products were obtained by calcination at 500 °C ($NiFe_2O_4$) and 600 °C ($CuFe_2O_4$) for 5 h. Silica template was removed by 2M NaOH (three times for 24 h at room temperature). TEM (Figure 5) and HRTEM analyses revealed that independently of the template used, obtained bimetal oxides show domains of the ordered 3-D pore structure inherited from the template. Calculated crystal sizes for $CuFe_2O_4$ and $NiFe_2O_4$ obtained from KIT-6 as template were about 6 nm and 9 nm respectively.

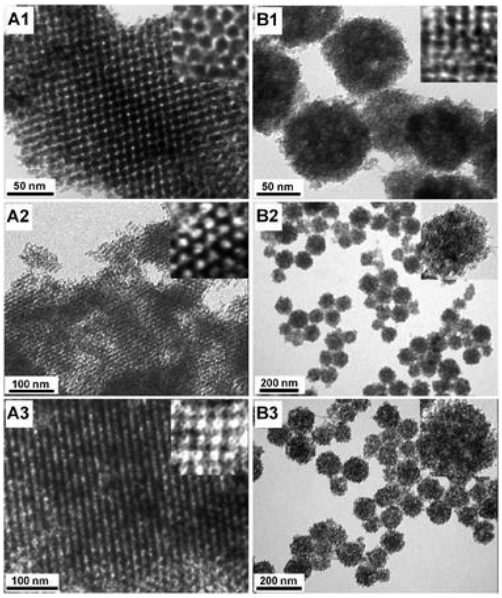

Fig. 5. TEM images of mesoporous bimetal oxide replicas prepared using KIT-6 (A1, A2, A3) silica and MCM-48 silica nanospheres (B1, B2, B3): (A1, B1) $NiFe_2O_4$, (A2, B2) $CuFe_2O_4$, (A3, B3) $Cu(20)/CeO_2$. Insets show high magnification images of the corresponding materials. Reprinted with permission from (Yen et al. 2011, [41]). Copyright 2011 The Royal Society of Chemistry.

$NiCo_2O_4$ [42] is an interesting complex oxide for applications in several fields: electrocatalysis, flat panel displays, drug delivery, optical limiters, chemical sensors, and so forth. The problem associated with the classical synthetic methods for this material are related to its instability at temperatures above 400 °C and the formation of undesirable phases like NiO or elemental Ni and Co during synthesis. The hard templated synthetic procedure for this material was conducted by preparing ethanol

solution of $Co(NO_3)_2x6H_2O$ and $Ni(NO_3)_2x6H_2O$ and mixing for 30 min with the silica templates (SBA-15 and KIT-6), after which the ethanol was evaporated overnight. The obtained precursor/template composite was calcined at 375 °C for 5 h, and at 550 °C for 4 h. Silica template was removed using 2M NaOH solution at 70 °C. In order to investigate the thermal stability of the product, dried mesoporous replicas were thermally treated once more at 550 °C for 4 h. Independently of the calcination temperature, obtained powders were indeed replicas of the template used (Figure 6). SBA-15 replicated material showed the existence of several hundred nanometers long nanowires with a diameter of 7 – 8 nm, which grew within the silica mesochannels (the pore size of template SBA-15 silica was 6 – 7 nm). In the case of KIT-6 replicas, the material consists of large 3D domains with their size being smaller than the template's particles (figure can be seen in the original paper [42]).

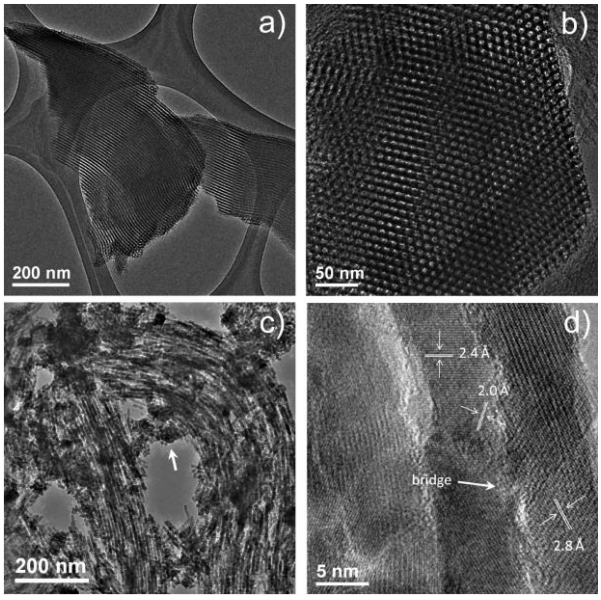

Fig. 6. TEM images of (a, b) SBA-15 silica, (c, d) SBA-15 templated NiCo2O4 (calcined at 550 oC). The arrow in (c) points to a group of randomly oriented nanoparticles. The d spacings of 2.8, 2.4, and 2.0 Å correspond to (220), (311), and (222), respectively, of the cubic NiCo2O4. Reprinted with permission from (Cabo et al. 2009, [42]). Copyright 2009 American Chemical Society.

Kaner, Mousavi et al. have fabricated highly ordered mesoporous $CuCo_2O_4$ nanowires by using mesoporous silica SBA-15 as a hard template for nanocasting [43]. In this work, they investigated performances and capability of mesoporous $CuCo_2O_4$ nanowires for energy storage and their potential application for developing the new generation of supercapacitors. By combining the features of transition metal oxides with a hard-template synthesis method for controlling the structure, they achieved a remarkable specific capacitance of 1210 F g^{-1} at a current density of 2 A g^{-1}, which overcomes the restriction of the current carbon-based supercapacitors.

Mesoporous metal oxides are a desirable material for application in VOCs sensing due to simple adjustment of their structure and morphology by modifying the synthetic methods. *V.K. Tomer* and *S. Duhan* have reported the nanocasting approach for fabrication of ordered mesoporous SnO_2/TiO_2 nanohybrids doped with Ag for the detection of ethanol [44]. The mesoporous silica SBA-15 was used as a hard template and the as-synthesized nanocomposites-based sensor showed high selectivity, sensitivity and a low detection limit for ethanol, with wide, 1 to 500 ppm detection range.

Hard template synthesis and applications of mesostructured carbon nanomaterials

The synthesis of porous carbon framework is also being performed through the nanocasting strategy where mesoporous silica, porous membranes or colloidal particles (or other patterned solids) serve as a hard template, which are removed after the synthesis. Carbon precursors mostly include polymerizable monomers (such as glucose, sucrose, and dopamine) and oligomers (phenolic oligomers), which exert an impact on the synthetic methodology and features of the final carbon support. In the case of the polymer as a carbon source, a considerable drawback is the low solubility and mobility of the polymer in solution, hindering the process of filling the polymer within the hard template.

In the recent study by *Birss et al.* two different ordered mesoporous carbons (OMCs) were synthesized using hexagonal mesoporous silica (HMS) as a hard template [45]. Anthracene (A) and sucrose (S) served as carbon precursors for the formation of OMC-A and OMC-S, respectively, and sulfuric acid was used as the catalyst for polymerization of these precursors. Upon polymerization, both OMCs were heat-treated at 1500 °C in a N_2 atmosphere. Contact angle kinetics (CAK) and water vapor sorption (WVS) methods investigated the wettability in detail, revealing that OMC-A was very hydrophilic whereas, unexpectedly, OMC-S turned out to be significantly more hydrophobic than OMC-A even though both materials were formed with the same HMS template. TEM tomography revealed for the first time the presence of a thin, hydrophobic, microporous carbon shell layer surrounding the mesoporous core of the OMC-S particles. This phenomenon could be attributed to the high polarity and affinity of sucrose and sulfuric acid to silica, which triggered the formation of a thin layer on the outer surface of HMS during the drying process and thus producing a carbon shell after carbonization.

Furthermore, the heat treatment made these materials more hydrophobic as it removed the oxygen groups. On the other hand, the internal mesopore structure of the as-synthesized OMCs remained hydrophilic because of the high density of surface oxygen groups inside the pores which originated from C-O-Si bond during the carbonization process. After the removal of the silica template, C-OH groups were left behind. This study showed the importance of carbon precursors` properties and their effect on the final carbon nanomaterial.

The development of different microwave absorbing materials has been of great interest for various applications and OMCs have shown high microwave absorbing properties and high efficiency for these applications. *Yuan et al.* synthesized an OMC by nanocasting with mesoporous silica SBA-15 as a hard-template [46]. The precursor was a sulfonated product of the pyrrole oligomer and the process was catalyzed by sulfuric acid, resulting in nitrogen and sulfur co-doped OMC with a homogeneous distribution of those heteroatoms. The synthesized material showed highly ordered

mesoporous structures, as well as a large surface area. Doping with N and S heteroatoms improved the surface activity and conductivity, which led to a good microwave absorption performance, wide absorption bandwidth and material with low density. The as-prepared material, at the thickness of 2.5 mm, showed a minimum reflection loss (RL) of -32.5 dB and an absorption bandwidth of 3.2 GHz (RL < −10 dB) in X-band (8.2–12.4 GHz). All of these properties support the possible utilization of these materials as high-performance microwave absorbers.

Porous carbon supports have become suitable materials for applications in catalysis due to their high surface-to-volume ratio and high structural stability. In the work of *Liu et al.* a polyacrylonitrile copolymer, poly(styrene-co-acrylonitrile) (PS-c-PAN), was used as both a carbon source and porogen for the preparation of hierarchical 3D porous carbon nanostructures [47]. PS part of the copolymer served as a soft template, being responsible for the formation of micro and mesopores, whereas the PAN part acted as a carbon source. In the synthesis, silica spheres as a hard template were filled with the PS-c-PAN copolymer dissolved in THF. Upon the evaporation of THF, stabilization and carbonization, the silica framework was removed, and the final three-dimensional porous carbon (3DC) was obtained (Figure 7). This material further served as a support for immobilization of Pt nanoparticles. The Pt nanoparticles were fabricated through borohydride reduction route in an ice-bath using H_2PtCl_6 as a Pt precursor and $NaBH_4$ as a reducing agent. TEM images show that 3DC has a macroporous inner structure with a narrow thickness of the wall, around 1-2 nm, and the size of macropores of around 150 nm, which are voids obtained after the removal of silica. Regarding the structure and surface of the 3DC material, N_2 adsorption/desorption isotherms indicated a Brunauer–Emmett–Teller (BET) surface area to be 550.5 $m^2\ g^{-1}$ and the existence of micro-, meso-, and macro-pores. XRD patterns of 3DC and Pt/3DC showed characteristic diffraction of graphitic carbon and characteristic diffraction peaks of face-centered-cubic (fcc) crystalline Pt, respectively. Furthermore, SEM image and energy dispersive spectrum (EDS) of Pt/3DC confirmed the presence of Pt, C, and O with a measured Pt atomic content of 13.19%. The obtained Pt/3DC assembly exhibited excellent electrocatalytic activity in the oxygen reduction reaction.

Direct methanol fuel cells (DMFC) are based on the catalyzed reaction of oxidation of methanol to carbon dioxide. Therefore, the process is highly dependent on the type of catalyst. Pt is typically used as a catalyst in both half reactions of DMFC due to its excellent activity at low temperature (below 80 °C). However several hindering facts still have to be overcome. In the work by *Macias-Ferrer et al.* a micro/nano-structured pyrolytic carbon (MNC) was prepared via a nanocasting method using SBA-15 as a hard template and refined sugar as a carbon precursor [48]. The synthesized carbon material served as a support for PtCo (atomic ratio 52:48) nanoparticles. The introduction of a second metal (Co) facilitates the oxidation of CO to CO_2, thus regenerating the active sites on Pt. The electrocatalytic activity of PtCo/MNC to methanol oxidation reaction (MOR) was evaluated through cyclic voltammetry (CV) by measuring the ratio between the forward peak maximum current density (If), and the backward peak maximum current density (Ib) denoted as If/Ib. The measured value showed that the newly synthesized PtCo/MNC was highly tolerant of CO poisoning, which is a significant step in the development of anodic catalysts for DMFC.

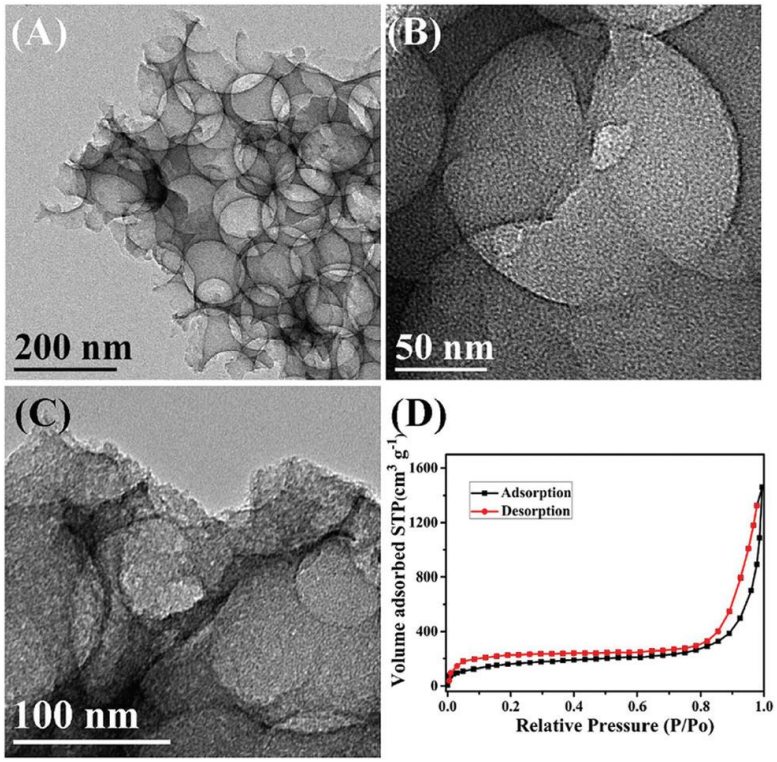

Fig. 7. (A–C) TEM images and (D) N_2 sorption isotherms of 3DC. Reprinted with permission from (Liu et al. 2018, [47]). Copyright 2011 The Royal Society of Chemistry.

The fact that a variety of volatile organic compounds (VOCs), many of which are toxic and hazardous, are emitted in the everyday indoor environment has attracted much attention in recent years. Various VOC sensing materials are being developed in order to construct portable gas sensors operating at around room temperature. Graphite-phase carbon nitride (g-C_3N_4 or g-CN) emerged as a suitable polymeric semiconductor, having a conjugated π-system and therefore a 2-D planar structure, high chemical stability, and a facile synthesis protocol. However, the utilization of the original g-CN material in sensing remained on backseat due to its several drawbacks such as low reactivity and small specific surface area. In the work by *Kienle et al.* m-CN doped with Pd-WO_3 nanocomposite was synthesized for the first time, using KIT-6 as a hard template. The material was showcased for efficient room temperature-sensing and detection of hazardous VOCs such as formaldehyde, toluene, acetone and ethanol that are usually found in the indoor environment [49]. Tungsten trioxide (WO_3) is a well-known n-type semiconductor with various tunable properties convenient in modulating the 2-D and 3-D materials for gas sensing. Moreover, Pd nanoparticles can create a synergistic effect of electronic and chemical sensitization. Characterization of the mentioned nanocomposite confirmed its high porosity, 3D cubic ordered mesoporous 2D layered architecture, high surface area, and uniform porous structure.

Supercapacitors have been largely investigated recently as a possible alternative to the conventional energy storage devices. However, several drawbacks such as low power density and specific capacitance at high current densities, and the lack of the life-cycle efficiency have to be overcome. In the study by *Vinu et al.* highly ordered 3D cage-type mesoporous carbon materials were synthesized via FDU-12 silica hard template approach with sucrose as a carbon precursor [50]. This synthetic approach was microwave-assisted, which altogether reduced the time of the synthesis. Powder XRD and microscopic techniques such as HR-TEM, HR-SEM, and N_2 adsorption-desorption techniques revealed that this novel carbon material showed a 3D porous mesostructure with tunable pore diameters (5.7 to 9.4 nm) and a large specific surface area. The supercapacitive property was determined using cyclic voltammetry, electrochemical impedance, and charge-discharge measurements. It was confirmed that the prepared cubic mesoporous carbon material showed a much higher capacitance value compared to that of hexagonally-ordered mesoporous carbon with large pore diameters, activated carbon, and carbon nanotubes. *Lozano-Castelló et al.* have synthesized mesoporous carbon thin film using an ordered mesoporous silica thin film as a hard template [51]. They have demonstrated that controlling the structure and morphology of carbon films contributes to an enhanced electrical conductivity of the material and their application as electrodes for micro-capacitors.

Conclusions and Perspectives

Hard template procedure is a highly effective methodology for the construction of different metal oxide and carbon-based mesoporous materials, with possible utilization of different types of templating mesoporous silica nanomaterials. The obtained materials have much higher surface area than the bulk material and hence more of the active interface area to interact with the environment. This feature is particularly attractive for applications in catalysis, through providing more of the active sites for reaction to occur. Also, the physicochemical properties are being modified with the transition of the material from bulk to mesostructured nanomaterial. Transition metal MOXs change their electric, magnetic, optical and other physicochemical properties as a function of their composition and morphology. These different characteristics enable their broad application potential in catalysis, gas sensing, energy conversion and storage (as electrode materials for batteries and supercapacitors), magnetic devices, and so forth. Transition MOXs, with 3*d*-shell electrons, are quite suitable for the production of highly attractive mesoporous structures with high surface area and connected pore network. The mesoporous nature of these materials can help in achieving superior properties and consequently, enable their efficient applicability.

In gas sensing application, sensitivity and fast response of the sensing device are highly dependent on the properties of the sensing layer containing MOX. For example, better performance of the sensor is expected if the material used as the sensing layer exhibits large surface to volume ratio, due to enhanced accessibility of the surface for both reducing and oxidizing gas molecules. Since most of the metal oxides work at high temperatures, it is particularly important as well to obtain a material with a thermally stable porous structure, to preserve the high surface area at sensor operating temperatures [52-54].

As for the energy storage application, the presence of mesoporous structures in MOX manifests in the improvement of the energy density capacity. *Wang et al*. showed

that the synthesis of highly ordered mesoporous Co_3O_4 utilizing mesoporous KIT-6 and SBA-15 silica template allowed the production of material with excellent electrochemical performance as an electrode material in lithium-ion batteries and supercapacitors [55]. For Dye-Sensitized Solar Cells (DSSCs) application it is of great importance to produce titania based materials with high crystallinity and specific surface area. Besides that, porosity plays a crucial role in their usage as photocatalytic material [56] and most recently in Perovskite Solar Cells (PSCs). Due to its large energy band gap, matched energy level and high carrier mobility, porous titania serves as charge-injecting and hole-blocking oxide. Therefore, the researchers typically focus on controlling the mesoporous networks of TiO_2 and using amphiphilic block copolymers and different templates allows fine-tuning of the size and morphology of titania nanoparticles [57-59]. The efficient and most frequently used method for obtaining titania materials is conventional sol-gel processes. Materials prepared in this manner, however, are prone to lose their porosity at higher temperatures because of the intrinsic crystallization process of the anatase phase [60, 61]. Hence, many efforts have to be done to improve existing synthesis procedures by adjusting various parameters to obtain materials with optimal porosity for desired applications above.

As different morphology leads to different characteristics of the materials, synthesis of the plethora of materials for a variety of applications, as overviewed above, is possible through the employment of hard template methodology. Accounting for the opportunity to use the same principle for construction of complex multicomponent metal oxides or doped carbon nanomaterials, which further enhance the attributes of the products, the exponential growth in the number and quality of the materials synthesized through the hard template procedure is expected in the future, leading to their efficient utilization in a variety of practical applications.

Acknowledgments

The authors acknowledge the financial support of the Ministry of Education, Science and Technological Development of the Republic of Serbia (project number III45007 SMS, KV and MPN, and III44006 NK).

References

[1] Y. Xie, D. Kocaefe, C. Chen, Y. Kocaefe: J Nanomater,2016 **(**2016), Article ID2302595.
[2] V. Malgras, Q. Ji, Y. Kamachi, T. Mori, Fa-Kuen Shieh, K. C.-W. Wu, K. Ariga, Y. Yamauchi: Bull Chem Soc Jpn, 88 (2015) 1171–1200.
[3] D. Gu, F. Schüth: Chem Soc Rev, 43 (2014) 313−344.
[4] Y. Ren, Z. Ma, P. G. Bruce: Chem Soc Rev, 41 (2012) 4909−4927.
[5] Y. Deng, J. Wei, Z. Sun, D. Zhao: Chem Soc Rev, 42 (2013) 4054−4070.
[6] G. Prieto, J. Zečević, H. Friedrich, K. P de Jong, P. E. de Jongh: Nat Mater, 12 (2013) 34−39.
[7] Y. Wan, D. Zhao: Chem Rev, 107 (2007) 2821-2860.
[8] G. J. de A. A. Soler-Illia, C. Sanchez, B. Lebeau, J. Patarin: Chem Rev, 102 (2002) 4093−4138.
[9] E. L.Crepaldi, G. J. de A. A Soler-Illia, D. Grosso, F. Cagnol, F. Ribot, C. Sanchez: J Am Chem Soc, 125 (2003) 9770-9786.

[10] (a) G. J. de A. A Soler-Illia, E. Scolan, A. Louis, P. A. Albouy, C. Sanchez: New J Chem, 25 (2001) 156-165. (b) D. Grosso, G. J. de A. A Soler-Illia, F. Babonneau, C Sanchez, P. A. Albouy, A. Brunet-Bruneau, A R. Balkenende: Adv. Mater., 13 (2001) 1085-1090. (c) G. J. de A. A Soler-Illia, A. Louis, C. Sanchez: Chem. Mater., 14 (2002) 750-759. (d) E. L. Crepaldi, G. J. de A. A Soler-Illia, D. Grosso, C. Sanchez: New J. Chem., 27 (2003) 9-13.
[11] J. Lee, J. Kim, T. Hyeon: Adv Mat, 18 (2006) 2073–2094.
[12] Y. Wan, Y. Shi, D. Zhao: Chem Comm, 38 (2007) 897–926.
[13] Y. Wan, H. Yang, D. Zhao: Acc Chem Res, 39 (2006) 423–432.
[14] N. Duc Hoa, N. Van Duy, N. Van Hieu: Mater Res Bull, 48 (2013) 440–448.
[15] B. Z. Tian, X. Y. Liu, H. F. Yang, S. H. Xie, C. Z. Yu, B. Tu, D. Y. Zhao: Adv Mater, 15 (2003) 1370-1374.
[16] F. Jiao, A. Harrison, J. C. Jumas, A. V. Chadwick, W. Kockelman, P. G. Bruce: J Am Chem Soc, 128 (2006) 5468-5474.
[17] X. Y. Lai, X. T. Li, W. C. Geng, J. C. Tu, J. X. Li, S. L. Qiu: Angew Chem, 119 (2007) 752-755.
[18] Y. Shi, B. Guo, S. A. Corr, Q. Shi,Y.-S. Hu, K. R. Heier, L. Chen, R. Seshadri, G. D. Stucky: Nano Lett, 9 (2009) 4215−4220.
[19] X. Sun, H. Hao, H. Ji, X. Li, S. Cai, C. Zheng: ACS Appl Mater Interfaces, 6 (2014) 401−409.
[20] M. Imperor-Clerc, D. Bazin, M. D. Appay, P. Beaunier, A. Davidson: Chem Mater, 16 (2004) 1813-1821.
[21] C. Dickinson, W. Zhou, R. P. Hodgkins, Y. Shi, D. Zhao, H. He: Chem Mater,18 (2006) 3088-3095.
[22] R. Ryoo, S. H. Joo, S. Jun: J Phys Chem B 103 (1999) 7743-7746.
[23] C. Yu, J. Fan, B. Tian, D. Zhao, G. D. Stucky: Adv Mater, 14 (2003) 1742-1745.
[24] F. Kleitz, S. H. Choi, R. Ryoo: Chem Commun, 17 (2003) 2136-2137.
[25] X. Deng, K. Chen, H. Tüysüz: Chem Mater, 29 (2017) 40−52.
[26] W. Stöber, A. Fink: J Colloid Interface Sci, 26 (1968) 62–69.
[27] F. Hoffmann, M. Cornelius, J. Morell, M. Fröba: Angew Chem Int Ed, 45 (2006) 3216 – 3251.
[28] Y. Wan, D. Zhao: Chem Rev, 107 (2007) 2821-2860.
[29] R. Narayan, U. Y. Nayak, A. M. Raichur, S. Garg: Pharmaceutics, 10 (2018) 118.
[30] D. Zhao, J. Feng, Q. Huo, N. Melosh, G. H. Fredrickson, B. F. Chmelka, G. D. Stucky: Science, 279 (1998) 548-552.
[31] F. Kleitz, D. Liu, G. M. Anilkumar, I.-S. Park, L. A. Solovyov, A. N. Shmakov, R. Ryoo: J Phys Chem B, 107 (2003) 14296-14300.
[32] J. Fan, C. Yu, F. Gao, J. Lei, B. Tian, L. Wang, Q. Luo, B. Tu, W. Zhou, D. Zhao: Angew Chem Int Ed, 42 (2003) 3146 – 3150.
[33] F. Schüt: Angew Chem Int Ed, 42 (2003) 3604 – 3622.
[34] M. Tiemann: Chem Mater, 20, (2008) 961–971
[35] G. S. Gallego, F. Mondragón, J. Barrault, J. M. Tatibouët, C. Batriot-Dupeyrat: Appl Catal A, 311 (2006) 164-171.
[36] R. Pereñeguez, V. M. Gonzalaz-delaCruz, A. Caballero, J. P. Holgado: Appl Catal B, 123 (2012) 324-332.
[37] W. B. Yue, W. Z. Zhou: Chem Mater, 19 (2007) 2359–2363.

[38] Y. Wang, X. Cui, Y. Li, L. Chen, Z. Shu, H. Chen, J. Shi: Dalton Trans, 42 (2013) 9448-9452.
[39] R. Zhang, P. Li, N. Liu, W. Yue, B. Chen: J Mater Chem A, 2 (2014) 17329–17340.
[40] M. M. Nair, S. Kaliaguine, F. Kleitz: ACS Catal. 4 (2014) 3837−3846.
[41] H. Yen, Y. Seo, R. Guillet-Nicolas, S. Kaliaguine, F. Kleitz: Chem Commun, 47 (2011) 10473–10475.
[42] M.Cabo, E. Pellicer, E. Rossinyol, O. Castell, S. Suriñach: M. D. Bar, Crystal Growth & Design, 9 (2009) 4814 – 4821.
[43] A. Pendashteh, S. E. Moosavifard, M. S. Rahmanifar, Y. Wang, M. F. El-Kady, R. B. Kaner, M. F. Mousavi: Chem Mater, 27 (2015) 3919–3926.
[44] V. K. Tomer and S. Duhan: J Mater Chem A, 4 (2016) 1033–1043.
[45] X. Li, F. Forouzandeh, T. Fürstenhaupt, D. Banham, F. Feng, S. Ye, D. Y. Kwok, V. Birss: Carbon, 127 (2018) 707–717.
[46] X. Yuan, X. Xue, H. Ma, S. Guo and L. Cheng: Nanotechnology, 28 (2017) 375705.
[47] M. Liu, J. Li, C. Cai, Z. Zhou, Y. Ling and R. Liu: Dalt Trans, 46 (2017) 9912–9917.
[48] D. Macias-Ferrer, J. A. Melo-Banda, R. Silva-Rodrigo, M. Lam-Maldonado, U. Páramo-García, J. Y. Verde-Gómez and P. Del-Ángel-Vicente, Catal. Today, (2018)
[49] R. Malik, V. K. Tomer, T. Dankwort, Y. K. Mishra, L. Kienle: J Mater Chem A, 6 (2018) 10718–10730.
[50] W. S. Cha, S. N. Talapaneni, D. M. Kempaiah, S. Joseph, K. S. Lakhi, A. M. Al-Enizi, D.-H. Park, A. Vinu: RSC Adv, 8 (2018) 17017–17024.
[51] S. Leyva-García, D. Lozano-Castelló, E. Morallón and D. Cazorla-Amorós: J Mater Chem A, 4 (2016) 4570–4579.
[52] T. Waitz, T. Wagner, T. Sauerwald, C.D. Kohl, M. Tiemann: Adv Funct Mater, 19 (2009) 653–661.
[53] N. D. Hoa, S.A. El-Safty: Chem Eur J, 17 (2011) 12896–12901.
[54] N. Duc Hoa, N. Van Duy, N. Van Hieu: Mat Res Bull, 48 (2013) 440–448.
[55] G. Wang, H. Liu, J. Horvat, B. Wang, S. Qiao, J. Park, H. Ahn: Chem Eur J, 16 (2010) 11020–11027.
[56] W. Dong, Y. Sun, C. Wee Lee, W. Hua, X. Lu, Y. Shi, S. Zhang, J. Chen, D. Zhao: J Am Chem Soc, 129 (2007) 13894-13904.
[57] H. Lu, K. Deng, N. Yan, Y. Ma, B. Gu, Y. Wang, L. Li: Sci Bull, 61 (2016) 778-786.
[58] A. Sarkar, N. Joong Jeon, J. Hong Noh, S. Il Seok: J Phys Chem C, 118 (2014) 16688−16693.
[59] X. Sun, J. Xu, L. Xiao, J. Chen, B. Zhang, J. Yao, S. Dai: Int J Photoenergy, 2017 (2017), 4935265
[60] D. Li, H. Zhou, I. Honma: Nat Mater, 3 (2004) 65-72.
[61] S. Y Choi, M. Mamak, N. Coombs, N. Chopra, G. Ozin: A Adv Funct Mater, 14 (2004) 335-344.